ULTRASONIC FLAW CHARACTERIZATION IN THE RESONANCE REGION BY THE BOUNDARY INTEGRAL EQUATION METHOD

L. W. Schmerr, Jr., C. Sieck
Ames Laboratory, DOE
Iowa State University
Ames, Iowa 50011

ABSTRACT

When the wavelength of the ultrasound being used to characterize a flaw is of the same order of magnitude as the flaw size, conventional low and high frequency scattering approximations fail. In this frequency range, called here the resonance region, numerical methods are necessary. Here we show that one such method, the Boundary Integral Equation (BIE) Method, is an effective tool for solving elastic wave scattering problems in the resonance region provided some important modifications are made in the method as used previously by other authors. To illustrate the BIE method, scattering from a cylindrical void in two-dimensions is considered. Comparisons are given with complimentary analytical and experimental results.

INTRODUCTION

With the development of wide band ultrasonic equipment in recent years, much attention has been given to the use of ultrasonic spectroscopy techniques to non-destructively characterize the physical properties of various types of defects in materials. However, little of this data can be used quantitatively until it is coupled with analytical-numerical techniques capable of predicting and classifying flaw scattering properties. In the size-frequency regime where the flaw size and ultrasonic wavelengths are comparable (called here the "resonance" region), low and high frequency approximations fail (1), (2) and one is forced to resort to numerical methods. The only two methods that currently appear viable for solving elastic scattering problems in the resonance region are the Transition Matrix (3), (4) and the Boundary Integral Equation (BIE) Method (5), (6). We will show that the BIE method provides a very effective method of solution for elastic wave scattering problems in this region provided some important modifications are made in the standard BIE formulations.

BIE Formulation - The BIE method consists of writing the solution to a flaw scattering problem in terms of an integral equation over the scattering surface. This integral equation is generated using a fundamental singular solution (Green's Function) for the surrounding media and is solved numerically by subsectioning the surface into patches and choosing simple piecewise representations for the unknown over these patches.

To illustrate the BIE formulation explicitly, consider the scattering of harmonic elastic waves from a flaw in two dimensions (Fig. 1). For this case we have (5)

$$aU_\beta(P)=U_\beta^{INC}(P)+\int_S[t^n_\alpha(Q)U_{\alpha\beta}(Q,P)-\Sigma^n_{\alpha\beta}(Q,P)U_\alpha(Q)]\; dS\;(Q)\quad(\beta=1,2)\qquad(1)$$

where U_β is the displacement of the medium in the X_β-direction due to an incident ultrasonic wave whose displacements are U^{INC}_β. The components of the stress vector are t^n_β on the surface S of a scatterer whose outward normal is $\underline{n}$ (Fig. 1). Point Q is a point of integration on S, and P is a general point that can be either interior to the scatterer, on the scatterer surface S, or exterior to the flaw. In these three cases, the value of "a" in e.g. (1) takes on the value of a=o, $a=\frac{1}{2}$, or a=1, respectively. The tensors $U_{\alpha\beta}$ and $\Sigma^n_{\alpha\beta}$ are related to the fundamental solution for an isotropic elastic solid (5), (7).

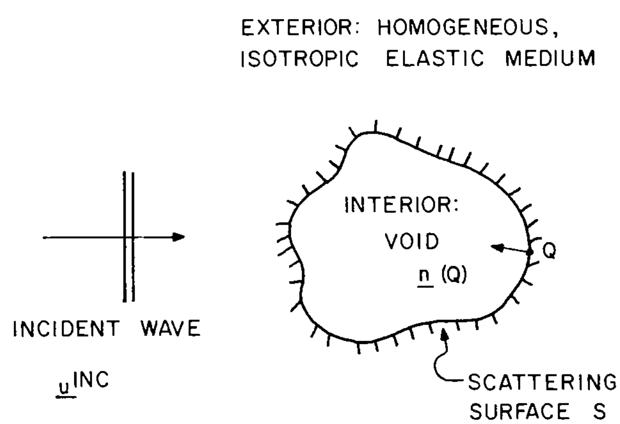

Fig. 1. Scattering geometry

When point P lies on the surface S of the scatterer, Eq. (1) is an integral equation for the unknown stresses and displacements on that surface. That equation can be solved by breaking the surface into straight segments Sn (n=1,2...N) whose centroids are located at points Pn, and assuming the tractions and displacements are constant over these segments. If Eq. (1) (with $a=\frac{1}{2}$) is then satisfied at N centroidal points Pm (m=1,2...N) on the surface, we obtain:

$$U_\beta(P_m)/2 = U_\beta^{INC}(P_m) + \Sigma_{n=1}^{n}\ t_\alpha^{n}\ (P_n) \int_{S_n} U_{\alpha\beta}(Q,P_m)dS(Q)$$

$$-\Sigma_{n=1}^{n}\ U_\alpha(P_n) \int_{S_n} \Sigma_{\alpha\beta}^{n}\ (Q,P_m)dS(Q)\ . \qquad (2)$$

Once the displacements or stresses are specified on the surface, Eq. (2) can be used to obtain a set of simultaneous equations for the remaining unknown surface quantities. These results and Eq. (1) (with a=1) may then be used to obtain the solution at any interior point in the solid. For example, if the flaw is a void, the stresses are zero on S and Eq. (2) becomes

$$\Sigma_{n=1}^{n}\ [\delta_{\alpha\beta}\delta_{mn}/2 + \int_{S_n} \Sigma_{\alpha\beta}^{n}\ (Q,P_m)dS(Q)]\ U_\alpha(P_m) =$$

$$U_\beta^{INC}\ (P_m)\ (m=1,2....N). \qquad (3)$$

This is standard BIE formulation which has been used recently by Tan (5), for example, to solve several elastic scattering problems. However, this method has a serious deficiency which was not mentioned in (5). This deficiency is that the approximate numerical solution [Eq. (3)] of Eq. (1) is inaccurate at certain characteristic frequencies. At those frequencies, non-zero fields can exist inside the flaw that do not satisfy Eq. (1), i.e., the left hand side of Eq. (1) is not zero when P is inside the scatterer, as it should be. These non-zero fields inside S cause large errors to occur in the solutions obtained from Eq. (3). To see this we have considered the scattering problem of cylindrical void in an otherwise homogeneous and isotropic elastic solid subjected to a plane incident compressional wave. Using a BIE computer code based on Eqs. (1) and (3), we calculated the far field radial displacement for the scattered waves at a 90^{o} orientation from the incident wave. The magnitude of this radial displacement as a function of frequency is shown in Fig. 2. In that figure we see an overall modulation as a function of frequency together with sharp peaks and dips (marked by arrows in Fig. 2). These rapid variations are not contained in the exact solution to this problem as can be obtained from a separation of variables solution (8). Similar extraneous variations in the frequency domain response also appear in acoustic and electromagnetic BIE formulations (9) and several means to eliminate them have been adopted. One method, which we have used successfully, (9), is to force the solution to zero at a specified number of points inside the scatterer, in order to better satisfy Eq. (1) when point P is inside S. This introduces addition constraints without adding additional unknowns so the system is then overdetermined, becoming:

$$\Sigma_{n=1}^{n}\ [a_m\delta_{\alpha\beta}\delta_{mn} + \int_{S_n} \Sigma_{\alpha\beta}^{n}\ (Q,P_m)dS(Q)]U_\alpha(P_n) =$$

$$U_\beta^{INC}\ (P_m)\ (m=1,2,M) \qquad (4)$$

where $a_m = \frac{1}{2}$ when $m \leq N$ and $a_n = 0$ when $m > N$.

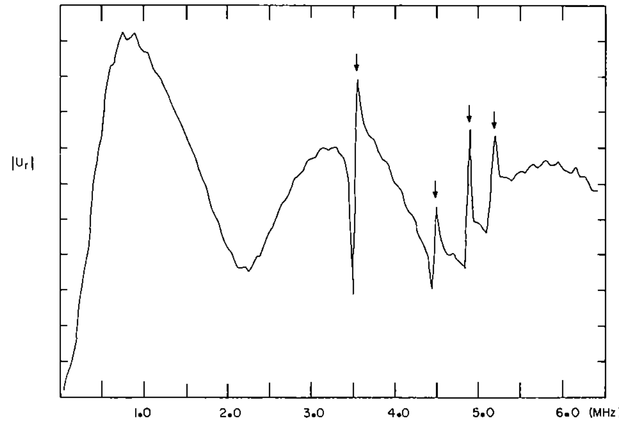

Fig. 2. Radial, far-field displacement at 90^{o} from incident wave, using unmodified BIE formulation.

If Eq. (4) is now solved in the least squares sense, we have found very good results can be obtained at all frequencies with as few as 3 extra equations. Figure 3 shows the same solution as Fig. 2 (solid line) and the solution to an overdetermined set of equations (squares) where Eq. (1) is satisfied at three arbitrary points inside the void. We see the overdetermined solution passes successfully through all the artificial peaks and dips and, in fact, is within several percent of the exact solution. As far as we are aware, this is the first time that this numerical problem with the BIE has been compensated for in this manner for elastic wave scattering problems.

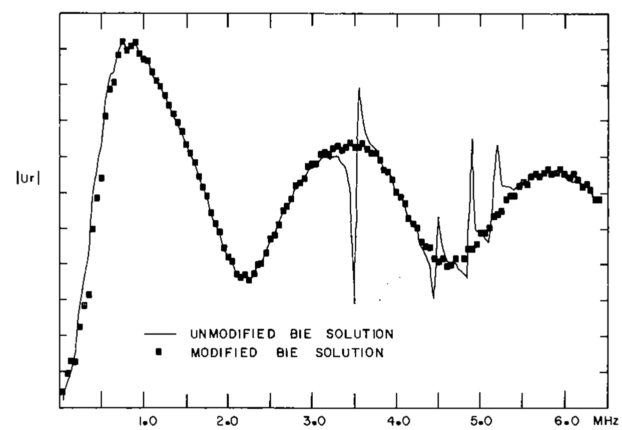

Fig. 3. Radial, far-field displacement at 90^{o} from incident wave. Modified and unmodified BIE formulations.

Experimental Comparisons - After developing an accurate working two-dimensional BIE computer code based on the modifications mentioned above, we have also tested it against complimentary experimental data. For example, as shown in Fig. 4, we machined the faces of an aluminum block at various angles from the top face and placed a through-drilled

1.59mm (1/16") diameter hole in the center of the block. The transmitter was a 10 MHz Panametrics broad-band compressional wave transducer that always remained fixed in location on the top face of the block while a matching receiving transducer was moved onto the various faces. Figure 5 shows the digitized transient response obtained from the receiver at angles of 45^{0}, 90^{0}, and 135^{0} from the transmitter. These responses show two major features: a large front surface reflection (A) and a smaller "creeping wave" contribution (B) which has been found previously by Sachse (10). This creeping wave contribution is basically a grazing incidence wave that wraps around the surface of the cylindrical hole, radiating in all directions. Since the path length and radiation loss grows as the angle between transmitter and receiver becomes smaller, we expect that the creeping wave contribution will become smaller and more separated from the front-surface reflection as the angle decreases, as in fact Fig. 5 demonstrates. The frequency components in the signals of Fig. 5 were computed using the Fast Fourier Transform capabilities of the data acquisition and processing system shown in Fig. 4. and the results are shown in Fig. 6 where we have plotted the magnitude of the Fourier transform of the responses at 45^{0}, 90^{0}, and 135^{0}, respectively. We see a distinct set of modulations in these frequency spectra, together with an overall envelope which is a function of the transmitting and receiving transducer characteristics. Using standard deconvolution techniques (11) to remove these transducer characteristics, we obtained a set of deconvoluted spectra whose magnitudes are plotted on a smaller frequency scale in Fig. 7. Also plotted in Fig. 7 is the magnitude of the radial displacement at the receiving transducer location as computed from the modified BIE formulation described previously. It is seen that within an arbitrary scale factor, both curves show the same overall types of modulation, except in the low frequency region where the deconvolution cannot be expected to be accurate since there is little energy content in the incident pulse.

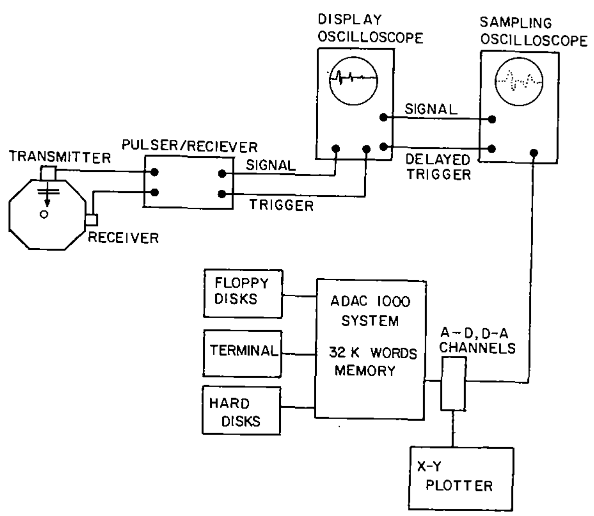

Fig. 4. System configuration.

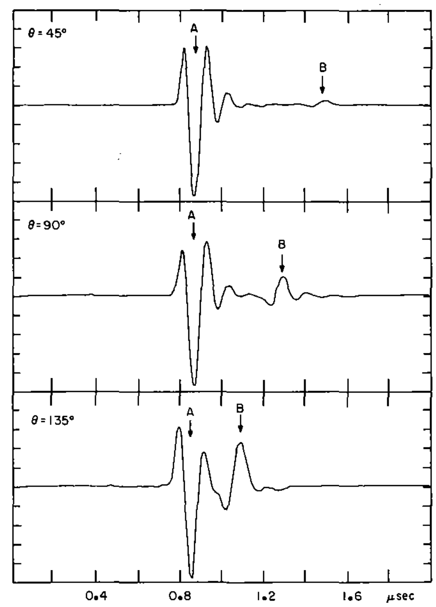

Fig. 5. Front surface and creeping wave contributions at 45^{0}, 90^{0}, and 135^{0} from transmitter.

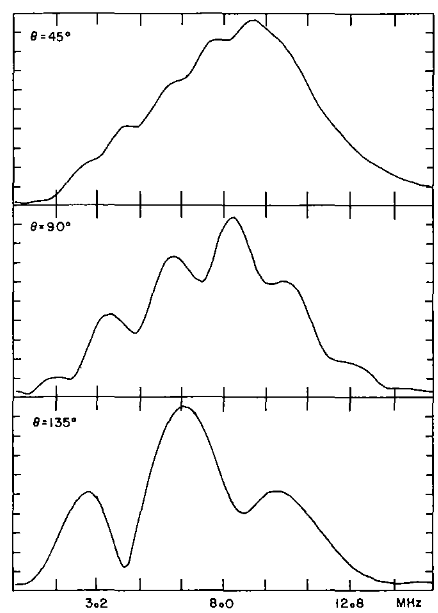

Fig. 6. Magnitude of Fourier transform of the response at 45^{0}, 90^{0}, and 135^{0} from transmitter.

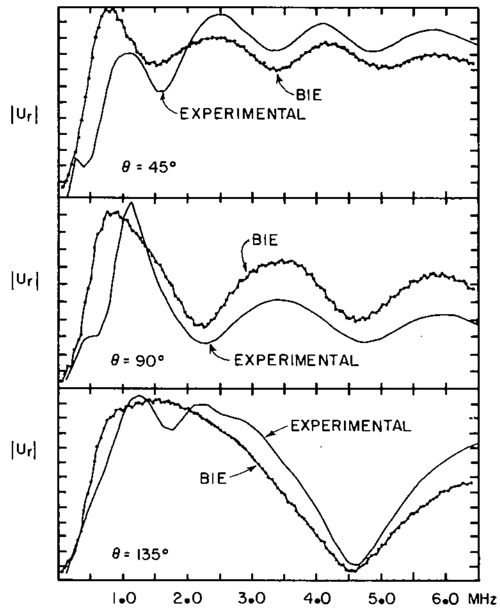

Fig. 7. Comparison of deconvoluted experimental spectral and BIE results.

One aspect of wave scattering experiments in elastic solids which is not found in analogous acoustic or electromagnetic problems is the phenomena of mode conversion between compressional and shear wave disturbances. Thus, when the incident compressional wave from the transducer of Fig. 4 strikes the side-drilled hole, both scattered compressional and shear waves are generated. This mode conversion process, although it makes elastic wave scattering problems more difficult than similar acoustic or electromagnetic cases, also offers the possibility of being used to extract additional information on a flaw's characteristics. These mode converted signals were picked up from the side-drilled hole of Fig. 4 with a 5MHz Parametrics shear wave transducer, producing the transient response shown in Fig. 8 when the receiving shear wave transducer is at 90^{0} from the transmitter. The frequency components of this signal were obtained and deconvolved to produce the spectrum shown in Fig. 9. In Fig. 9, the magnitude of the far-field tangential displacement at the receiving transducer location is also plotted from the results of our BIE code. Again, the comparison between the experimental and numerical results is very good to within an arbitrary scale factor.

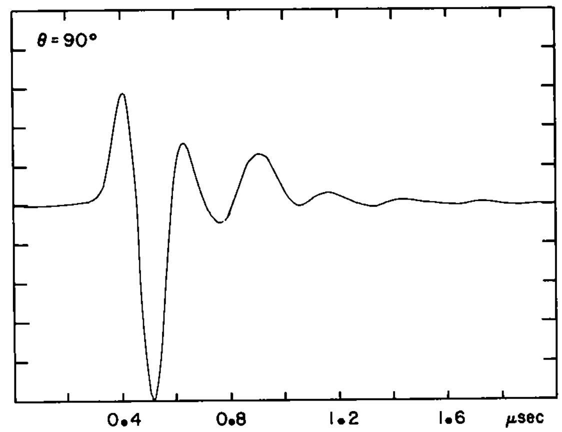

Fig. 8. Scattered shear waves at 90^{0} from compressional wave transmitter.

Concluding Remarks - The strength of the BIE approach lies in the fact that it is capable of handling complex flaw geometrics and of working effectively in the resonance region where other methods fail. With some modification, the model presented here can also be applied to three-dimensional voids, inclusions, and cracks and to surface and near-surface flaws as well. Currently, efforts are underway to make these modifications and extensions of the technique. Perhaps the single major disadvantage of the BIE method is that it must obtain a separate solution for each frequency. Thus, over a wide range of frequencies, many solutions are needed. However, BIE solutions are within the capability of many dedicated minicomputer systems currently on the market, so that this limitation can, to some extent, be overcome without incurring excessive computer time costs. In fact, all the results obtained in this paper were computed on the microcomputer based data acquisition and processing system of Fig. 4.

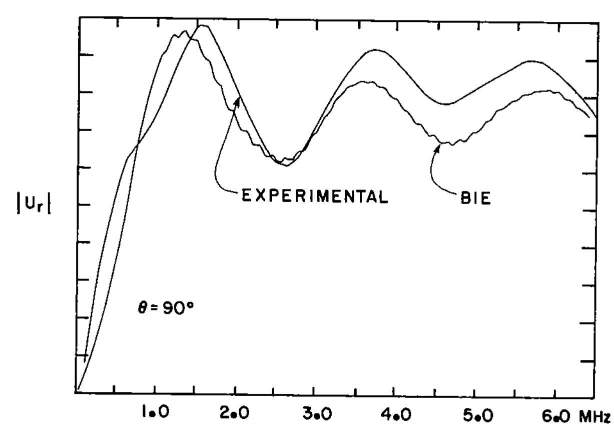

Fig. 9. Comparison of experimental and BIE results for the scattered shear wave.

ACKNOWLEDGEMENTS

This work was supported partially by the National Science Foundation through Grant No. ENG 77-06970 and the Engineering Research Institute of Iowa State University. The U.S. Department of Energy, through Contract No. W-7405-Eng-82, Office of Basic Energy Sciences, Division of Materials Sciences (AK-01-02), provided partial support for the development of the software used in this program.

REFERENCES

1. J. E. Gubernatis, E. Domany, and J. A. Krumhansl, "Elastic wave scattering theory with application to nondestructive evaluation", Los Alamos Scientific Laboratory, LA-UR-79-2393, 1979.

2. J. D. Achenbach, A. K. Gautesen, and H. McMaken, "Application of elastodynamic ray theory to diffraction by cracks" Modern Problems in Elastic Wave Propagation, Ed. by J. Miklowitz and J. D. Achenbach, John Wiley, NY, 219-238, 1978.

3. Y. H. Pao, "The transition matrix for the scattering of acoustic waves and for elastic waves", Modern Problems in Elastic Wave Propagation, Ed. by J. Miklowitz and J. D. Achenbach, John Wiley, NY., 123-144, 1978.

4. P. C. Waterman, "Matrix theory of elastic wave scattering", J. Acoust. Soc. Am. 60, 567-580, 1976.

5. T. H. Tan, "Scattering of elastic waves by elastically transparent obstacles (Integral Equation Method)", Appl. Sci. Res. 31, 29-51, 1975.

6. Y. A. Pao and V. Varatharajulu, "Huygen's Principle, radiation conditions, and integral formulas for the scattering of elastic waves", J. Acoust. Soc. Am. 59, 1361-1371, 1976.

7. A. C. Eringen and E. S. Suhubi, Elastodynamics, Vol. 2, Academic Press, NY, p.435, 1975.

8. Y. H. Pao and C. C. Mow, "Diffraction of elastic waves and dynamic stress concentrations", Crane-Russak, NY, pp.239-253, 1973.

9. H. A. Schenck, "Improved integral formulation for acoustic radiation problems", J. Acoust. Soc. Am. 44, 41-58, 1968.

10. Y. H. Pao and W. Sachse, "Interpretation of time records and power spectra of scattered ultrasonic pulses in solids", J. Acoust. Soc. Am. 56, 1478-1486.

11. E. Nabel and E. Mundry, "Evaluation of echoes in ultrasonic testing by deconvolution", Materials Evaluation 36, 59-77, 1978.

SUMMARY DISCUSSION

Jim Rose (University of Michigan [now Ames Laboratory]): Essential reduction in the number of terms in your matrix over the T-matrix?

Lester Schmerr (Iowa State): You're asking are the matrices used smaller?

Jim Rose: Can you get as good results resolution as their results with essentially smaller matrices?

Lester Schmerr: I have not done a direct comparison, but I think probably the order of magnitude is pretty much similar. What you need here is about 10 elements per wavelength to do a good job. By a good job I mean within a couple percent of the exact solution. So if you translate that up into whatever ka value that you want, I think the methods come out fairly comparable.

Vasundara Varadan (Ohio State): I wish to make some comments. The first problem that you showed that had the interior resonances in the scattered data was an exact boundary integral solution, but when you introduced an extra point which is in the interior of the scatterer, what you did is exactly the T-matrix method, using the extension theorum. So what you have really done is the T-matrix calculation using local basis function rather than global functions, which is the method I used when I showed the stress concentration factor results. One might also profit from looking at the electromagnetic literature. They don't call it the boundary method there, but the moment method. They were always plagued by the interior resonances, but they have found ways of getting around that problem. I don't know how complicated they are, but they have found ways of getting around that calculation. But the last calculation you showed is the T-matrix function, using local basis function.

Lester Schmerr: I mentioned there are other ways of handling that problem of the fictitious resonances. You can modify the integral equation that you start out with, and you get an integral equation which you can show is unique at all frequencies, even the frequencies of the interior problem, the complementary problem - that's been done in the electromagnetic and acoustic cases and worked there, so I don't see any reason why it wouldn't work here.

But you end up dealing with more complicated expressions, so I think it's more convenient to do it this way.

James Krumhansl, Chairman: Opsal.

Jon Opsal (Lawrence Livermore Laboratory): I don't know if I have the right picture of the problem, I feel like I'm missing something. You said that the field inside the void in a solid material and fields inside the void ought to be zero, at least the displacement fields?

Lester Schmerr: Yes.

Jon Opsal: What's the reason for that? There is nothing in the boundary condition that show they vanished, and if I just move inside -

Lester Schmerr: The integral relationships tell you it should be zero.

James Krumhansl, Chairman: The sum of the two terms should be.

Lester Schmerr: You basically cancel off the incident wave.

Jon Opsal: It has to be cancelled by the scattered field. I'm thinking of the scattered field.

Lester Schmerr: The scattered field is the negative of the incidence. As a matter of fact, if you calculate the displacements at an interior point inside the void when you're away from those interior resonances, you get something like 1 percent of 10 percent or less than your incident wave. But as soon as you get near the resonance, it becomes the same order of magnitude.

SUMMARY DISCUSSION

John Richardson (Science Center): Suppose you have a very tenuous inclusion instead of a void. Suppose you take a limit of the inclusion that essentially becomes increasingly tenuous.

Lester Schmerr: The inclusion will have a real resonance.

John Richardson: Then you let the inclusion become increasingly tenuous until it becomes a vacuum. You end up with a finite displacement field inside.

Lester Schmerr: I have not seen anyone use that limiting process. That might be possible.

James Krumhansl, Chairman: Visscher.

William Visscher (Los Alamos Scientific Laboratory): What do you do about the problem of singularity in fields?

Lester Schmerr: That's a good point. In doing the integrations, you have to evaluate them as principal value integrals, but because you have an explicit expression for the singularity, you can do the principal value integrations exactly.

William Visscher: I can see how that will work if you have certain symmetries, but for generally shaped surfaces?

Lester Schmerr: It doesn't depend on what the symmetry is because you locally have, basically, a flat element and you have the Green's Function for the infinite media.

James Krumhansl, Chairman: The approximation is essentially a flat element. Each one of those elements are treated in that way.

Lester Schmerr: Yes.

Vasundara Varadan: I have one more comment to make regarding computing complex resonances. We have, in fact, used some of these T-matrix ideas and calculated the resonance frequency for an oblate spheroid, elastic one, immersed in water. And these calculations are very, very expensive. We are searching all over for the complex plane for these resonance frequencies. What we found when we looked at complex resonance frequencies reflected in the form function of the scattered field amplitude as a function of frequency was that the resonances that are really deep in the complex plane do not show up in the product of the scattering cross section as a function of frequency. And we found it's only those resonance frequencies that have a real part quite near the real axis that are important. In fact, people at the Naval Research Laboratory, without any justification, have been doing these types of calculations for a long time. They can predict the resonant frequencies of many arbitrary shaped obstacles quite nicely, but what, in fact, they are predicting are only those frequencies. And they can pick those up quite easily from the scattering cross-section as a function of Ka.

Lester Schmerr: Can I make a point here? It is very expensive if you try to do any locating of these resonances in a complex frequency plane. There is a method called Prony's where you can extract those directly from time response, A-scan response. That's much less expensive, if it works.

Unidentified Speaker: We find it's very sensitive to the number of elements you use in Prony's method.

Lester Schmerr: We have tried that in a one-dimensional natural scattering system, and it does work pretty well. You have to be careful when you go from electromagnetic and acoustic to these problems here. Noise levels, for example, are different, especially underwater acoustics, for example. They are terrible. So -

James Krumhansl, Chairman: We'll move on. Very stimulating talk, obviously.